Recovering Handset Diversity and MIMO Capacity With Polarization-Agile Antennas

David G. Landon, *Student Member, IEEE*, and Cynthia M. Furse, *Senior Member, IEEE*

***Abstract*—Design guidance is provided for multiple-input–multiple-output (MIMO) antenna systems on handsets—a strong prospect for next generation wireless devices. Handheld wireless devices are likely to be rotated out of their optimal polarization, thereby experiencing significant power losses. An existing polarization-agile antenna design and a novel four-spoke extension recover significant fractions of the rotation-induced losses both in switched-antenna diversity and capacity calculations—all but 1 dB of diversity gains at a 99% system reliability, half of the C_E losses or 80% of the $C_{0.1}$ losses. These gains benefit four- and ten-element arrays and remain significant in the presence of −6 dB cross coupling and in volume-restricted arrays. Diversity order investigations also demonstrate a new, non-Rayleigh locus of curves describing patch antennas subject to rotation.**

***Index Terms*—Adaptive arrays, antenna arrays, diversity methods, multiple-intput–multiple-output (MIMO), polarization.**

I. Introduction

MULTIPLE-INPUT–MULTIPLE-OUTPUT (MIMO) systems offer increased throughput (channel capacity) for a fixed communication bandwidth and have received enthusiastic attention over the past decade since Foschini's seminal treatment [1]–[27]. Ironically, in an effort to better understand the multiplexing gains offered by MIMO, a normalization to the average *detected* power has been used that masks more dominant effects and can lead to false predictions of gains [15]. With proper normalization to the average impinging power based on an extension of [22], it becomes clear that MIMO systems deployed on portable handsets have much to gain from switched polarization diversity. Transceiver signal strength to or from a portable handset is subject to large variations due to the "essentially random orientation" typical of their use [4] and the resultant polarization mismatch between the handset antenna and the impinging wavefronts. Handset orientations in the horizontal plane are arguably fairly uniform over the full 360° range, a fact well represented by typical modeling efforts. But elevation angles also vary widely between a person looking up and looking down while holding a portable device and are typically not aligned with zenith. A representative elevation angle of 30° away from zenith was used in [5] to accurately model the way large mobile devices of past decades were held, but it is not as accurate a model for the smaller phones of today that are often held even closer to horizontal. Further, common usage of a cell phone includes tilting the head to either side to hold it against a shoulder or switching from the right hand to the left depending on user preference. It is easy to see that a handheld device would be subject to polarization mismatch losses resulting from random orientation relative to the fixed base-station transceiver.

Numerous researchers have addressed exploiting dual-polarized channels to mitigate wireless channel fades [6]–[10]. These studies have assumed that the relative orientation of the receiver and transmitter is constant or at least carefully constrained. Kozono, for example, considers a variable orientation for the receiver, but only within a fixed plane. The literature has largely assumed fixed orientations for receiver and transmitter—most often vertical dipoles and boresighted patch antennas [11]–[14], [24]. Li's work [16] involving azimuthal rotation of an array offers a rare exception to this pattern, but even this example preserves polarization alignment. In a significant departure from this pattern of fixed orientations, Cox carefully examines the value of using angular diversity to mitigate the effects of polarization mismatch due to handset rotation [4]. Little interest persisted for the topic and there is no comparable study applied to MIMO signaling. As one would expect, MIMO capacity also suffers when handset arrays are subjected to the random orientation typical of their use.

This paper synthesizes an inexpensive solution to recover a significant fraction of these capacity losses. Marrying the idea of antenna subset selection [17], [18] and polarization-agile antennas [19], [20], one arrives at a polarization-selectable approach of great value both to MIMO systems and to single-input–single-output (SISO) systems. Fundamental contributions of this paper include the following: 1) quantitatively demonstrating that the typical assumption of a receiver with fixed orientation is very inaccurate for predicting the capacity of handheld MIMO wireless devices, 2) significant recovery of the capacity and diversity losses from parallel array element designs through switchable polarization-agile elements, 3) a novel four-spoke extension of the three–spoke polarization-agile design in [20], 4) scalability to larger array sizes, and 5) less loss through cross coupling and limited array sizing than traditional array designs. Section II outlines how to compute the diversity gains that rotation-diverse antennas offer leading to the simulated results of Section III. Section IV describes how to compute comparative capacity studies for the same antenna arrays leading to simulated results in Section V.

Manuscript received January 2, 2007; revised July 18, 2007.

D. G. Landon is with the Electrical and Computer Engineering, University of Utah, Salt Lake City, UT 84112-9206 USA and also with the L3 Communications, Salt Lake City, UT 84116-0850 USA.

C. M. Furse is with the Center of Excellence for Smart Sensors and the Electrical and Computer Engineering, University of Utah, Salt Lake City, UT 84112-9206 USA and also with the LiveWire Test Labs, Inc., Salt Lake City, UT 84117 USA (e-mail: cfurse@ece.utah.edu).

Color versions of one or more of the figures in this paper are available online at http://ieeexplore.ieee.org.

Digital Object Identifier 10.1109/TAP.2007.908828

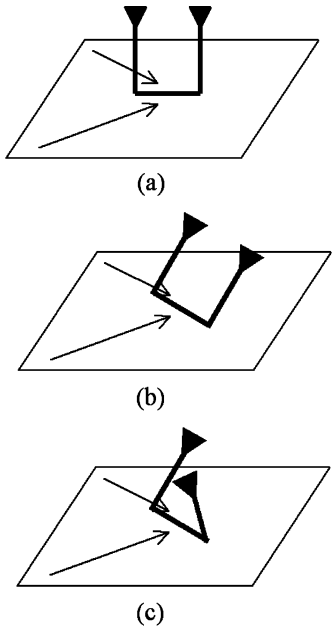

Fig. 1. Antenna rotations (solid lines with triangles on top) relative to the plane of incidence which includes two randomly oriented impinging signals (arrows): (a) parallel elements oriented normal to the plane of propagation, (b) rotated (tipped) parallel-element antenna array, and (c) polarization-diverse antenna array.

II. Computation of Diversity Gains for Rotation-Diverse Antennas

This section extends on methods used in [4] to explore orientation-degraded diversity gains and demonstrates an unexpected result: Patch antennas and dipoles are quite different in their diversity behavior, although both antenna types perform far below the idealized model assuming perfect polarization alignment that [4] reports for dipoles. These results are preparatory to a study of a switchable antenna design to mitigate these losses as discussed in the following section.

Fig. 1(a) depicts a typical antenna diversity scenario. Two parallel dipoles are oriented normal to the plane of propagation in which predominantly reflected and scattered copies of the transmit signal intermingle. The receive antennas are spaced sufficiently (typically, $\lambda/2$) to see statistically uncorrelated superpositions of the impinging waves. By switching on just the antenna that perceives the largest signal strength, one significantly lowers the probability of signal outage, a drop in signal strength sufficient to overcome the system link margin and terminate reliable communication.

Receive diversity has long been used to improve a system's resistance to fading, but the use of parallel dipoles is of limited value against rotation–induced outages typical of cell phone operation. As depicted in Fig. 1(b), use of parallel antennas allows a system to choose from independently faded antenna signals, but both are subject to the same polarization mismatch losses. Instead, it is more appropriate to use antennas with diverse orientations as depicted in Fig. 1(c) [4]. Indeed, Cox demonstrates that such an approach offers diversity gains of 10 dB or more for a pair of dipoles depending on the outage definition (tolerable probability of unusably low signal levels), number of antennas, and power combining method [4].

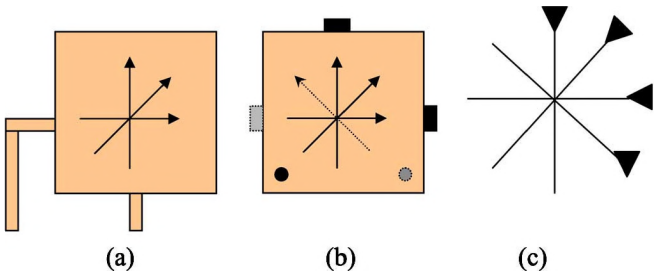

Fig. 2. Polarization-agile antennas: (a) dual-fed patch, (b) extension (gray elements) on the design from [20] in which filled rectangles are PIN diodes, feeds are at bottom corners, and polarization modes are given as arrows, and (c) four rotated dipoles.

Subsequent sections will demonstrate even further gains at little additional cost by the extension of Cox's angular diversity to "polarization-agile" [19] angular diversity. Replacing each simple dipole in Fig. 1(c) with a switchable antenna, such as those depicted in Fig. 2, considerably lessens the possibility of system outage. Only a 3-D polarization-agile design can switch to closely align to an arbitrary linear polarization, so some losses will not be recovered with these planar designs. However, significant size and cost advantages make a planar design very attractive. The dual-fed patch antenna of Fig. 2(a) transmits or receives 0° or 90° linear polarization, depending on which feed port is activated. The polarization-agile antenna of Fig. 2(b) has a single feed (a black circle) and two positive intrinsic negative (PIN) diodes (black rectangles) to switch between 0°, 45°, or 90° linear polarization [19], [20]. The novel addition of a second PIN diode and feed point (shown in gray) would allow for an additional polarization axis at 135°, an axis that proves to be useful in switched attempts at recovering polarization mismatch loss. Similarly, the four dipoles of Fig. 2(c) sweep out linear polarizations of 0°, 45°, 90°, and 135°, though the four-point feeding is more cumbersome than for the patch antennas of Fig. 2(a) and (b). Throughout this paper, the selectable polarization orientations will be referred to as spokes with the obvious connection to the spokes of a bicycle wheel. In this paper, the gain patterns of the n-spoke antennas are all modeled as though they had the same gain pattern and were then appropriately rotated to each of $n, 180°/(n-1)$ spaced orientations. Such a model might be reexamined in future work, but is sufficiently accurate for this study.

The same simulation environment described by Cox [4] can be used to demonstrate a simple method of recovering a considerable fraction of the losses he reports. The environment is simulated as a set of $N = 30$ impinging plane waves arriving in a single horizontal plane. The kth wavefront has a Rayleigh-distributed magnitude A_k, uniformly distributed angle of arrival (AOA) φ_k, and uniformly distributed phase β_k. Assuming that the antenna sets are uniformly spaced at the phase center by $\lambda/2$ along a line (somewhat greater than in [4] to better accommodate MIMO), the ith antenna set sees a path-length adjustment to the phase term leading to a composite phase term ψ_{ki}, where $\psi_{ki} = \beta_k + \pi(i-1)\cos\varphi_k$. The magnitude A_k is also adjusted

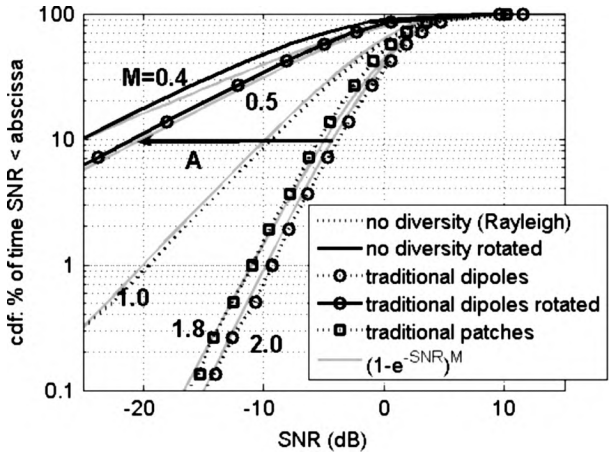

Fig. 3. SNR cdfs via selection diversity for rotated (solid curves) and idealized, unrotated dipole arrays (dashed curves). A single half-wavelength dipole represents the "no diversity" case and follows a Rayleigh distribution when unrotated. The gray curves are taken from (2) and express the effective diversity order as the exponent M showing very close agreement between the simulated and theoretical results. Notice that the diversity order ratio of $2.0/0.5 = 4$ indicates that the traditional dipoles cdf curve can be computed as the cdf of a pair of rotated dipoles raised to the fourth power. Thus, a pair of dipoles subject to random rotation has only 25% of the effective diversity order typically predicted by traditional (unrotated) models.

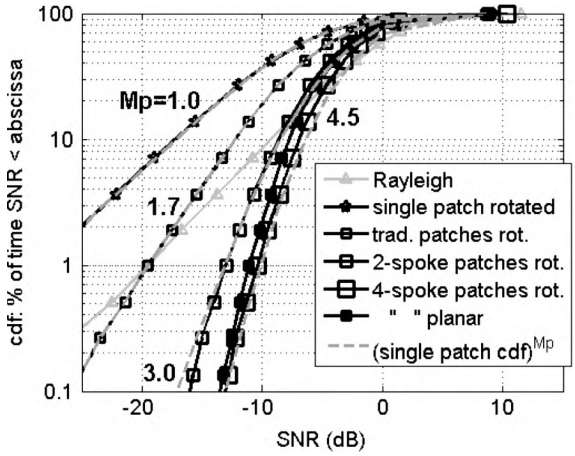

Fig. 4. SNR cdfs via selection diversity for polization-agile, two-element array designs computed over 20 000 simulated environments. "Rayleigh" is a single vertical dipole, which clearly does not provide an accurate model for nondipole antenna models. "Single patch rotated" is a single $\lambda/2$ patch. The other orthogonally oriented patch pairs are endowed with two or four spokes [see Fig. 2(b)] in "two-" and "four-spoke patches rotated" and reconstrained to be coplanar in "four-spoke patches rotated, planar." The dashed curves represent an exponentiation of the data in the "single patch rotated" curve and represent the effective diversity order relative to this single rotated patch. Notice, as in Fig. 3, that each curve can be computed from any other by raising exponentially the cdf values in the base curve to the ratio of their Mp values. "Four-spoke patches rotated" is the design offering the best diversity gain with only minor degradation when constrained to be fully planar.

for any polarization mismatch via the dot product $\vec{P} \cdot \vec{E}$ between $\vec{P}$, the unit normalized vector describing the orientation of the linear wavefront polarization and $\vec{E}$, the electric field vector of the antenna transmit beam pattern. The dependence of $\vec{E}$ on the elevation θ_k and azimuth φ_k is given as $\vec{E}(\theta_k, \varphi_k)$ in (1), and the field is normalized to unit power radiation for the antenna. Assuming that the waves are all vertically polarized in the horizontal plane, $\vec{P}$ would simply be $\hat{z}$ and θ_k would always be $\pi/2$. Instead, it is computationally convenient to hold the orientation of the antennas fixed and rotate the horizontal plane about them. This, in turn, varies the wavefront polarization vector and makes the dot product less trivial. The preceding definitions enable the following statement of the voltage V_i detected at the ith antenna [4]

$$V_i = \sum_{k=1}^{N} (\vec{P} \cdot \vec{E}(\theta_k, \varphi_k)) A_k \exp(j\psi_{ki}). \tag{1}$$

Analytical expressions for the E-field of an ideal $\lambda/2$–dipole or patch antenna exist (see [4, eq. (3)] and [21, eq. 5.73)]). However, to enable eventual comparisons of ideal antennas with other practical designs, a numerical method is preferred. Each antenna is assumed perfectly matched.

Under switched power combining, only the antenna with the largest detected V_i is activated. This does not achieve a power gain from coherent combining, but is inexpensive, simple, and effective in achieving much of the available diversity gain. To compute the signal-to-noise ratio (SNR) reported in Figs. 3 and 4, one may compute the signal power as $|V_i|^2$, and the SNR is the ratio of this signal power to some fixed noise level N_0. Recognizing that all curves will eventually be normalized by a common average SNR value, one may arbitrarily choose $N_0 = 1$. These methods will be used in the following section to explore diversity implications of different array designs.

III. Switching Polarization-Agile Antennas Improves Diversity Gains

The simulation framework outlined in Section II is now applied to demonstrate the degree to which a switched polarization-agile antenna approach can recover significant portions of SISO signaling SNR losses that result when a handset antenna is subject to random orientations. Subsequent sections will address MIMO issues.

To produce each of the figures of this section, 20 000 random environments are generated and normalized as in [22] to the average power detected by a reference dipole antenna as it is swept over a 50-λ range of locations. Whenever the polarization of the impinging fields is unknown, an additional sweep of antenna orientations is made to find the best polarization alignment for the spatial sweep of the reference antenna. Each figure reports the likelihood that the SNR achieved by a certain antenna array design via selection diversity exceeds a given level. For comparison, theoretical curves are included for the probability Ps that the SNR under selection combining is below the specific value "SNR," for M equal-mean, Rayleigh-distributed branch power signals (see [23, eqs. (8.4.14) and (8.4.15)])

$$\begin{aligned} \boldsymbol{Ps} &= (\mathbf{1} - \boldsymbol{e}^{-\mathbf{SNR}})^{\boldsymbol{M}} \\ &= (\text{single branch Rayleigh cdf})^{M}. \end{aligned} \tag{2}$$

The second half of (2) is a reminder that Ps is simply the cumulative density function (cdf) of the Rayleigh distribution raised to the Mth power. The simulated and theoretical curves in Fig. 3 agree very well for dipoles, suggesting that a single dipole and a pair of dipoles, respectively, achieve roughly 0.4 and 0.5 effective orders of diversity [22] when subject to rotation. This indicates a very significant loss in diversity order from 2 to 0.5

for the traditional paired dipoles and has severe consequences for the outage probabilities of a randomly oriented handset using two parallel dipoles. Traditional antennas perform very poorly when subject to random handset orientation. The simulated curves for a single vertical $\lambda/2$–dipole, labeled "no diversity," and the pair of parallel vertical dipoles, labeled "traditional dipoles," assume the idealized fixed orientation imposed in most modeling and measurement campaigns. This fixed orientation assures optimal alignment with the polarization of the fixed base station, so these curves easily beat their rotated counterparts "no diversity rotated" and "traditional dipoles rotated," which are randomly oriented relative to the same 20 000 simulated environments. When concerned with communication system link-budget specifications for sufficient power to guarantee 90% link reliability (the SNR falls below this level only 10% of the time), the fixed orientation of typical models predicts 17.5 dB of SNR unavailable to mobile users with randomly oriented devices (see marker A in Fig. 3). For a 99% reliability, the "traditional model" is 28 dB overly optimistic.

In fixed orientations—"traditional dipoles" versus "traditional patches" in Fig. 3—dipoles outperform patches with effective diversity orders of 2.0 and 1.8, respectively. Each pattern is normalized to unit-power radiation, but a greater fraction of the patch pattern is directed above and below the horizontal plane—a fact that proves advantageous when rotation is included in Fig. 4, but which does not help in the unrotated case. In the fixed orientation, average collected power is tied to the path integral of the E-field in polar coordinates

$$\int_0^{2\pi} |E_\theta(\theta=\pi/2,\varphi)|^2 + |E_\varphi(\theta=\pi/2,\varphi)|^2 \, d\varphi. \quad (3)$$

For a dipole with unit power radiation, this path integral is 0.83, while the same integral around a bottom-fed patch parallel to the yz-plane is 0.66. The ratio of these powers is 1.26 or 1.00 dB explaining the observed dipole advantage at the cdf = 50% level in Fig. 3. Of course, nearly 3 dB of the energy from a dipole may be absorbed in the user's head, more than erasing this apparent advantage. The backplane of the patch prevents much loss of energy into the user's head and should allow patches to outperform dipoles in handset designs—a subject for later research.

A comparison of the dipole results of Fig. 3 with those computed for patch antennas in Fig. 4 indicates that diversity gains depend heavily on antenna type. The curve "traditional patches rotated" in Fig. 4 is a pair of coplanar, vertical, bottom-fed, $\lambda/2$-square patch antennas commonly considered for MIMO applications in handsets. The curve falls well within the dipole curves "traditional model" and "traditional model rotated" of Fig. 3, suggesting that patches are both less benefited by optimal alignment and less penalized by rotation than dipoles are. In particular, for a 90% reliability, patches would outperform dipoles by 8 dB. (Interestingly, pairing a patch and dipole antenna in a single array design—not shown—does not exhibit greater gains than those achieved by patches alone.)

This less extreme behavior is reflected in a rather different shape for the patch curves as compared to the dipole curves—an effect easily missed if tempted to directly compute the diversity effect through determining the near-equal eigenvalues of the correlation matrices for each curve as in [22]. The "traditional patches rotated" curve has a much steeper slope and a different curvature than the "Rayleigh" curve in Fig. 4 or any of the curves in Fig. 3. Although these curves are quite different from the dipole curves, the patch curves are closely related to each other. While brute-force simulation does not reveal what analytical function describes the cdf of the "single patch rotated curve," the other patch curves are clearly well estimated by an exponential function of this data: "(single patch cdf) ^{Mp}." The exponent Mp can be interpreted as an effective diversity order relative to a single rotated patch and demonstrates the expected result that switched diversity offers nearly a twofold (1.7-fold) increase in the effective diversity order for paired versus single patches. A comparison with (2) indicates that this model is identical to that given for dipoles, except that it is based on a different fundamental curve, namely, the single patch cdf.

Fig. 4 demonstrates considerable further gains available from using switchable, polarization-agile elements in devices with random orientations. A rotated pair of "two–spoke patches" such as those shown in Fig. 2(a) or (b) offers an effective diversity order of 3.0, while the rotated pair of "four-spoke patches" achieves an effective diversity order of 4.5. This level is very near the idealized cdf curve of the "traditional dipoles" in Fig. 3 and little additional improvement is possible for twofold selection diversity combining even when the spoke count is increased beyond four. Of course, the dual ports of Fig. 2(b) required to enable a four-spoke design are costlier than using only one port to support a two- or three-spoke design. This latter inexpensive design was computed as "three-spoke patches rotated" but is not shown in Fig. 4. It falls roughly halfway between the "two-" and "four-spoke..." curves just discussed and offers an excellent hardware cost versus performance compromise. Depending on the cost tradeoffs, switched polarization-agile antennas can inexpensively restore all but about 1 dB of the diversity losses for a 99% reliable system. This means that link budgets for the "four-spoke patches rotated" design need only to add 1 dB of power rather than the 28 dB needed for the two-dipole "traditional model rotated" design when a handset is subject to the rotation typical of cell phone use.

Recognizing that many portable device designers will be unhappy to accommodate the dimensions of two orthogonal patch antennas, the final black curve, "four-spoke patches, rotated, planar" illustrates the value of using the four-spoke design of Fig. 2(b) with two coplanar patches. This penalizes the orthogonal "four-spoke patch rotated" design by 0.5 dB but continues to considerably outperform the polarization-nonagile design given by "traditional patches." Dipole designs matching Fig. 2(c) are also simulated but excluded from these plots, because the cost of providing four ports is prohibitive with no promise of benefit beyond that offered by the polarization-agile patches.

It is apparent that diversity gains of traditional antenna arrays are severely penalized when random orientation is included in modeling handset use. These penalties can be largely overcome with the novel extension to existing polarization-agile designs in Fig. 2(b) or slightly less benefit (roughly 1 dB) by limiting the design to use just one feed port. In Sections IV and V, these designs will be shown to aid MIMO system objectives as well.

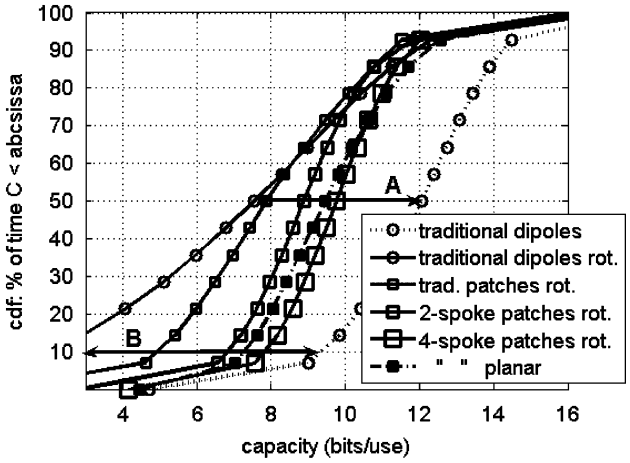

Fig. 5. Capacity cdfs for switched, angle-diverse array designs. The "four-spoke patches rotated" design achieves capacities higher than other designs both for mean and outage capacity definitions.

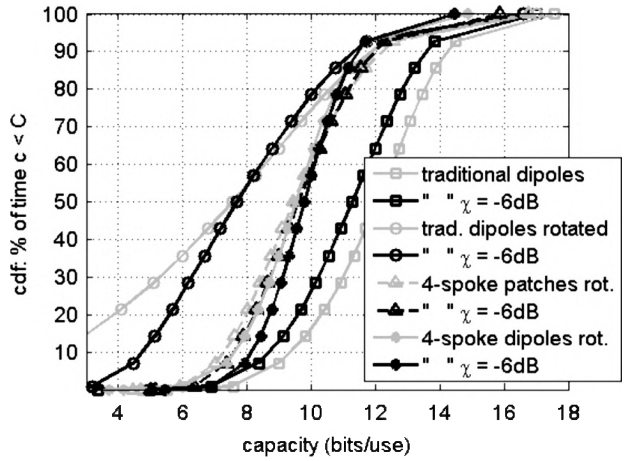

Fig. 6. Consequences on switched-antenna capacity of -6 dB channel polarization cross coupling. Cross polarization modestly impacts the four-spoke designs but actually benefits the "traditional dipoles rotated" case by virtually guaranteeing polarization alignment to at least a part of the signal.

IV. Switched MIMO Capacity Computation and Normalization

MIMO systems also exhibit losses due to polarization misalignment and can benefit in similar fashion to the SISO results seen in Section III from the inclusion of polarization-agile elements. Unlike in Section III, these gains involve the simultaneous activation of multiple antennas. This section describes how to model these MIMO capacities in advance of demonstrating various simulation results in Section V. Successful MIMO communication relies on achieving sufficiently unique superpositions of the transmitted signals arriving at each of the receive elements and is often realized with sufficient antenna spacing at both the base station and the mobile. Limitless space is assumed at the base station or "transmit side" to realize this ideal—typically 10–20λ is sufficient on elevated platforms. In Figs. 5 and 6, the number of transmitter and receiver antennas, N_T and N_R, respectively, are $N_T = N_R = 2$. Thus, the independent transmit signals are simply modeled as two sets of realizations of the AOAs φ_{k1} and φ_{k2}, magnitudes A_{k1} and A_{k2}, and phase variables β_{k1} and β_{k2}. This allows for the computation of a matrix of V_i's: $[V_{i11}, V_{i12}; V_{i21}, V_{i22}]$ based on using two active elements—one spoke from each of the two polarization-agile antennas on the handset. This matrix V_i actually represents an instance of the narrowband channel matrix H from the MIMO literature [2], [27] relating the input and output bit streams x and y, respectively, as $y = Hx$.

For each simulated instance of H, an instantaneous estimate of the channel capacity is computed via the waterfilling algorithm described in [2], [25], and [27]. Although asymptotically optimal selection methods exist for receiver subset selection of two active elements among the many spokes [18], [30], the problem is small enough to compute the capacity for each spoke pairing and the largest value is selected. The Ergodic capacity C_E is then estimated as the average capacity over an ensemble of Hs. Other statistics, such as outage capacities defined at a 1% ($C_{0.01}$) or 10% level ($C_{0.1}$), may be extracted from the capacity cdf. One might be tempted to reduce simulation complexity by focusing only on maximizing the strength of the signal at each antenna. However, this per-element maximum power selection algorithm led to inferior capacities by nearly 1 b/use in Fig. 5 near marker A and was discarded.

The most common normalization in the MIMO literature dictates that on a per-channel basis the detected voltage gains represented by H are scaled by some value α to achieve an average unity power constraint $(1/(N_T N_R)) \sum_{i=1}^{N_T} \sum_{j=1}^{N_R} |\alpha H_{ij}|^2 = 1$. Equivalent formulations involve an expectation operator or a Frobenius norm [15]. Such a normalization allows for a comparison of systems based on detected SNR and is reasonable for comparison of systems that collect RF energy in exactly the same way—as is true in many signal processing studies. However, when comparing antennas with differing abilities to extract energy from a channel (as is true of the polarization-variable antennas in this paper), antennas should be favored if they consistently extract more useful energy. Normalizing to the average *detected* power inappropriately gives preference to uniform subchannel strengths $|V_{i11}| \approx |V_{i12}| \approx |V_{i21}| \approx |V_{i22}|$—even when these subchannels are uniformly poor—and leads to absurd results. For example, normalization to *detected* power suggests incorrectly that the capacity of planar, polarization-nonagile antenna arrays subject to handset rotation roughly matches that of optimally oriented planar arrays and that polarization-agile antennas considerably outperform optimally oriented arrays.

To correctly see the advantage of the optimal polarization alignment mentioned previously, one must normalize to some metric related to the *available* power. A review of the curves "traditional model" and "traditional model rotated" in Fig. 3 shows that the strongest V_i detected in the "traditional model" with its optimal polarization alignment is 7–10 dB stronger at least 60% of the time than the strongest voltage detected by the rotated version of the array. Thus, if the "traditional model" detects an SNR of 20 dB, the "traditional model rotated" should detect an average SNR of less than 13 dB—a loss that translates into a 7–10-dB link margin error completely missed by the traditional normalization. At high SNR, a capacity-maximizing H of dimension $N_R = N_T = 2$ achieves an average or ergodic capacity of $2 \log_2$ (SNR) b/s/Hz [1] (or bits per use when

considering a matched-filtered communication approach typical of digital communications [27]). Thus, proper normalization to available power for this capacity-maximizing H yields a capacity of $2\log_2$ (13 dB) = 8.8 b/use in the rotated antenna case—well below the polarization aligned capacity of $2\log_2$ (20 dB) = 13.3 b/use. Proper normalization can be achieved by reusing the approach of [22] as described in Section III. Simulated noise is then added to set the average SNR to 20 dB in the investigations of Section V.

V. Switching, Polarization-Agile Antennas Improve MIMO Capacity

The same polarization-agile designs that recovered diversity losses in Section III can recover capacity losses not typically modeled in MIMO systems. The traditional configuration of two parallel dipoles demonstrates these losses well. The polarization-aligned "traditional dipoles" support a capacity of C_E = 12 b/use, a value that drops to just 7.5 b/use when subject to random orientation in "traditional model rotated" (see Fig. 5, marker A). Outage capacity losses are even more severe (see Fig. 5, marker B) though the outage capacity is much less catastrophic for patches subject to rotation than for dipoles. At an outage likelihood of 10% (90% reliability), for example, patches outperform dipoles with a capacity of 5.5 b/use as compared to just 2.2 b/use for the "traditional model rotated." Both fall far below the 9 bits/use predicted by the perfectly oriented "traditional model."

The curves "two–" and "four–spoke patches rotated" represent the improved capacities achieved by n-spoke switched patch antennas based on designs depicted in Fig. 2(a) and (b). Using two spokes recovers 25% of the C_E losses indicated by marker A of Fig. 5. Using three spokes increases this to 40% recovery (not shown in Fig. 4), while increasing the count to four spokes achieves 50% recovery of the C_E losses. Moving from four to eight spokes only adds another 0.1 b/use (also not shown) indicating that four spokes is a point of diminishing return. This is fortuitous as it is not clear that a patch with more than four spokes could be constructed. From a system design perspective, dropping to three-spokes might be a prudent choice. A pair of three-spoke patches offers 0.3 b/use less than a pair of four-spoke patches, but it requires just one feed port rather than two (and an associated power splitter) as depicted in Fig. 2(b). Recovery of outage capacity $C_{0.1}$ is even more impressive. Where the traditional dipole model predicts $C_{0.1}$ = 9 b/use, only 2.2 b/use are available under rotation (see Fig. 5, marker B). Nearly 5.5 b/use are recovered with four-spoke patches for a recovery of 80% of the rotation-induced losses.

Of course, the two– and four–spoke designs described previously require 3-D designs using two orthogonal, polarization–agile patches. As this leads to a size that may be undesirably large, a four–spoke dipoles, rotated planar (not shown) and "four–spoke patches, rotated planar" design were considered. The planar four–spoke dipoles, rotated design loses 1.9 b/use for a 10% outage probability ($C_{0.1}$) relative to the 3-D, orthogonally placed "four–spoke dipoles, rotated" design. The significant outage penalty must be carefully weighed against the improved 3-D footprint of the device. The differences between

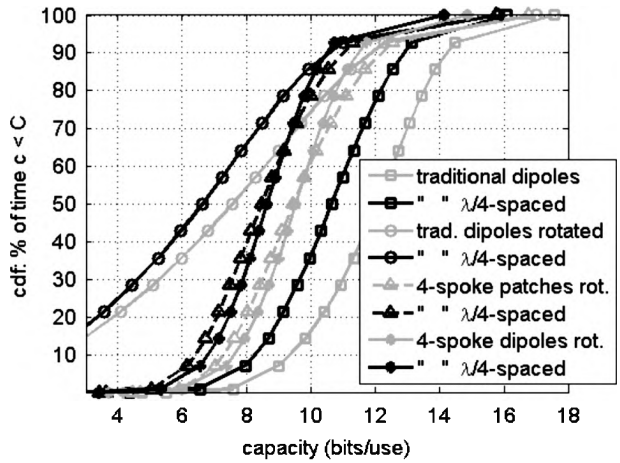

Fig. 7. Consequences of limited element spacing ($\lambda/4$) on the capacity of switched antenna designs, named as described in Fig. 5. Limited spacing hurts both idealized and polarization-agile antennas by reducing signal decorrelation.

the orthogonal and planar patch designs are less significant. C_E for the "four–spoke patches, rotated planar" design only beats that of the "four–spoke patches rotated" by 0.1 b/use and $C_{0.1}$ for the planar design is only 0.7 b/use worse, making it much more reasonable to trade the capacity losses of this planar design for its smaller size. Interestingly, if an array consists of two patches, each with a single feed, the coplanar configuration is consistently better than the orthogonal configuration.

Channel depolarization can limit or destroy capacity gains available through orthogonal polarization channels [15], so it is important to consider its impact on these designs as well. Wireless channels often exhibit a cross coupling of as much as −6 dB [6]–[26]. Fig. 6 indicates that cross coupling, as modeled in the straightforward extension of (1) given in [4, eq. (11)] and [15], does not uniformly impact the capacity of the various designs. Cross coupling has a large and consistently negative impact on the idealized models "traditional model" and "traditional model rotated." The mean capacities of traditional patches (not shown) and "traditional dipoles $\chi = -6$ dB" indicate a loss of 0.8 b/use. This reflects the impossibility of aligning simultaneously to both co- and cross-polarized components of the signal—a fact that is overlooked using the *standard normalization* [15]. In contrast, the outage capacity $C_{0.1}$ of the rotated dipoles antennas increases from less than 2 b/use to nearly 5 b/use, reflecting the fact that a nonnegligible cross-coupled signal is detectable even when the array is completely misaligned with the orientation of the stronger polarization component. However, cross coupling has little impact on the polarization-agile design curves. The average capacity of "four-spoke dipoles rotated $\chi = -6$ dB" and "four-spoke patches rotated $\chi = -6$ dB" improve slightly by 0.2 b/use and remain the appropriate design choices in the presence of channel cross coupling. The outage benefit is greater for dipoles than for patches due to the difference in their gain patterns.

Although the switched, multispoke design is primarily intended to recover rotation-induced losses exhibited by standard array designs (parallel elements targeting spatial diversity), linking polarization with MIMO often suggests the contrasting idea of a compact design based on colocated elements. Fig. 7

illustrates the impact of cutting the spacing in half between these multispoke antenna designs to $\lambda/4$. Because the entire array is ideally positioned on a handset above the region obstructed by the user's hand, current cell phone frequencies near 1800 MHz may allow such a design to fit on wireless-enabled electronic organizers. The width of a planar pair of $\lambda_{\text{air}}/4$ patches spaced at their centers by $\lambda_{\text{air}}/4$ is $\lambda_{\text{air}}/2 = 8.3$ cm—a much better fit than the 12.4 cm otherwise needed for a spacing of $\lambda_{\text{air}}/2$. Of course, MIMO may first be truly practical for cell phones and other small handhelds when a higher frequency like 5.2 GHz allows this same dimension to drop to 2.9 cm. Unlike the previous study of nonzero cross polarization, all of the curves in Fig. 7 are penalized by the consequent increase in the correlation of the MIMO subchannels. The "traditional model $\lambda/4$-spaced" degrades by more than 1 b/use to $C_E = 10.4$ b/use and the polarization-agile designs by about 0.6 b/use to $C_E = 8.6$ b/use as seen in "four-spoke patches rotated $\lambda/4$-spaced" and "four-spoke dipoles rotated $\lambda/4$-spaced." Cutting the spacing more may be unrealistic, since the spokes or patches in either set would begin to overlap (even a $\lambda/4$-spacing is only possible when the dielectric constant of the patch substrate sufficiently shortens the carrier wavelength). Of course, the novel addition of a second port to the design in Fig. 2(b) opens up the possibility of using two colocated polarization subchannels to achieve MIMO diversity. This approach may be worth exploring in a later work—[15] indicates that some channels perform equally well with either colocated polarization diversity or spatial diversity—but using two ports to create independent orthogonal channels would limit the number of distinct polarization dimensions available to either port.

A final study demonstrates extensions of switched polarization-agile antennas to larger numbers of antennas ($N_T = N_R = 4$ and 10) and to an investigation of the gains available at other SNR levels. It is found that where the traditional model offers a capacity bounded by $C_E = N_R \log_2$ (SNR) [1], the four-spoke design achieves $0.8\ N_R \log_2$ (SNR) rather than the $0.65\ N_R \log_2$ (SNR) achieved by the polarization-nonagile traditional designs.

VI. Conclusion

MIMO antenna systems on handsets are likely to be rotated out of the optimal polarization alignment typically imposed in both modeling and measurement campaigns, thereby experiencing significant power losses. A correct capacity normalization relative to available power demonstrates the value of using switched, polarization-agile antennas. They inexpensively recover half of the C_E losses and three-fourths of the $C_{0.1}$ losses. Polarization misalignment power losses also plague SISO designs leading to a 17–28-dB link-margin penalties for dipole-based systems (losses are less severe for patch antennas). Polarization-agile antennas can recover all but 1 dB of switched-antenna diversity gains in systems requiring 99% link reliability. Antenna type is also shown important to SISO diversity with coplanar agile and nonagile patches outperforming their planar dipole counterparts by 8 dB or more. This is a diversity order gain of roughly 4 based on a traditional Rayleigh-based locus of curves for dipoles or a new cdf-based locus of curves for patches.

A novel four-spoke version of a three-spoke polarization-agile antenna is introduced and shows moderate performance gains over the original three-spoke version. Still, cost and complexity concerns may lead to more common use of the three-spoke version. Channel-induced polarization cross coupling of -6 dB has little impact on the capacity achieved by these polarization-agile designs. In contrast, because of their reliance on spatial diversity, they are penalized by reduced interelement spacing—albeit, by less than traditional parallel dipoles are for the same reduction in spacing (1 b/use). The benefits of polarization-agile antennas are also found to scale with array element count, offering $0.8\ N_R \log_2$(SNR) rather than the $0.65\ N_R \log_2$(SNR) achieved by traditional arrays subject to handset rotation even for large numbers of array elements.

Switched polarization-agile antennas are demonstrably better than nonswitched solutions in every comparison except cost and complexity. But even cost and complexity differences almost disappear when considering the single-port three-spoke patch design. In both MIMO and SISO systems subjected to high variations in orientation, it offers vastly improved diversity and capacity gains for minimal cost, making its deployment an attractive choice both for legacy and next generation handset designs.

References

[1] G. J. Foschini and M. J. Gans, "On limits of wireless communications in a fading environment when using multiple antennas," *Wireless Personal Commun.*, vol. 6, pp. 311–355, Mar. 1998.

[2] D. Gesbert, M. Shafi, D. Shiu, P. J. Smith, and A. Naguib, "From theory to practice: An overview of MIMO space-time coded wireless systems," *IEEE J. Sel. Areas Commun.*, vol. 21, no. 3, pp. 281–302, Apr. 2003.

[3] D. Tse and P. Viswanath, *Fundamentals of Wireless Communication*. Cambridge, U.K.: Cambridge University Press, 2004.

[4] D. C. Cox, "Antenna diversity performance in mitigating the effects of portable radio telephone orientation and multipath propagation," *IEEE Trans. Commun.*, vol. COM-31, no. 5, pp. 620–628, May 1983.

[5] O. P. Gandhi, G. Lazzi, and C. Furse, "Electromagnetic absorption in the human head and neck for mobile telephones," *IEEE Trans. Microw. Theory Tech.*, vol. 44, no. 10, pp. 1884–1897, Oct. 1996.

[6] W. C.-Y. Lee and Y. S. Yeh, "Polarization diversity system for mobile radio," *IEEE Trans. Commun.*, vol. COM-20, no. 5, pp. 912–923, Oct. 1972.

[7] S. Kozono, T. Tsuruhara, and M. Sakamoto, "Base station polarization diversity reception for mobile radio," *IEEE Trans. Veh. Technol.*, vol. VT-33, no. 4, pp. 301–306, Nov. 1984.

[8] R. G. Vaughan, "Polarization diversity in mobile communications," *IEEE Trans. Veh. Technol.*, vol. 39, no. 3, pp. 177–186, Aug. 1990.

[9] C. B. Dietrich, K. Dietze, J. R. Nealy, and W. L. Stutzman, "Spatial, polarization, and pattern diversity for wireless handheld terminals," *IEEE Trans. Antennas Propag.*, vol. 49, no. 9, pp. 1271–1281, Sep. 2001.

[10] J. Shi, A. Shah, and A. Abidi, "Performance of dual polarized antennas in PCS 1900 MHz systems," *Proc. IEEE Veh. Tech. Conf.*, vol. 2, pp. 1186–1190, May 1997.

[11] R. U. Nabar, H. Bölcskei, V. Erceg, D. Gesbert, and A. J. Paulraj, "Performance of multiantenna signaling techniques in the presence of polarization diversity," *IEEE Trans. Signal Process.*, vol. 50, no. 10, pp. 2553–2562, Oct. 2002.

[12] C. Oestges, V. Erceg, and A. J. Paulraj, "Propagation modeling of MIMO multipolarized fixed wireless channels," *IEEE Trans. Veh. Technol.*, vol. 53, no. 3, pp. 644–654, May 2004.

[13] R. M. Narayanan, K. Atanassov, V. Stoiljkovic, and G. R. Kadambi, "Polarization diversity measurements and analysis for antenna configurations at 1800 MHz," *IEEE Trans. Antennas Propag.*, vol. 52, no. 7, pp. 1795–1810, Jul. 2004.

[14] P. Kyritsi, D. C. Cox, R. A. Valenzuela, and P. W. Wolniansky, "Effect of antenna polarization on the capacity of a multiple element system in an indoor environment," *IEEE J. Sel. Areas Commun.*, vol. 20, no. 6, pp. 1227–1239, Aug. 2002.

[15] D. Landon and C. Furse, "Inclusion of cross-coupling in MIMO normalization," *IEEE Trans. Antennas Propag.*, submitted for publication.

[16] X. Li and Z.-P. Nie, "Effect of array orientation on performance of MIMO wireless channels," *IEEE Antennas Wireless Propag. Lett.*, vol. 3, no. 1, pp. 368–371, Dec. 2004.
[17] S. Sanayei and A. Nosratinia, "Antenna selection in MIMO systems," *IEEE Commun. Mag.*, vol. 42, no. 10, pp. 68–73, Oct. 2004.
[18] A. Gorokhov, D. Gore, and A. Paulraj, "Receive antenna selection for MIMO spatial multiplexing: Theory and algorithms," *IEEE Trans. Signal Process.*, vol. 51, no. 11, pp. 2796–2807, Nov. 2003.
[19] S. Gao, A. Sambell, and S. S. Zhong, "Polarization-agile antennas," *IEEE Antennas Propag. Mag.*, vol. 48, no. 3, pp. 28–37, Jun. 2006.
[20] P. M. Haskins and J. S. Dahele, "Compact active polarisation-agile antenna using square patch," *Electron. Lett.*, vol. 31, no. 16, pp. 1305–1306, Aug. 1995.
[21] W. L. Stutzman. *Antenna Theory and Design*. New York: Wiley, 1998.
[22] O. Nørklit, P. Teal, and R. Vaughan, "Measurement and evaluation of mutli-antenna handsets in indoor mobile communication," *IEEE Trans. Antennas Propag.*, vol. 49, no. 3, pp. 429–437, Mar. 2001.
[23] R. Vaughan and J. B. Andersen. *Channels, Propagation and Antennas for Mobile Communications*. London, U.K.: The Institution of Electrical Engineers, 2003.
[24] J. W. Wallace, M. A. Jensen, A. L. Swindlehurst, and B. D. Jeffs, "Experimental characterization of the MIMO wireless channel: Data acquisition and analysis," *IEEE Trans. Wireless Commun.*, vol. 2, no. 2, pp. 335–343, Mar. 2003.
[25] G. G. Raleigh and J. M. Cioffi, "Spatio-temporal coding for wireless communication," *IEEE Trans. Commun.*, vol. 46, no. 3, pp. 357–366, Mar. 1998.
[26] J. W. Wallace and M. A. Jensen, "Modeling the indoor MIMO wireless channel," *IEEE Trans. Antennas Propag.*, vol. 50, no. 5, pp. 591–599, May 2002.
[27] M. A. Jensen and J. Wallace, "A review of antennas and propagation for MIMO wireless communications," *IEEE Trans. Antennas Propag.*, vol. 52, no. 11, pp. 2810–2824, Nov. 2004.
[28] J. J. A. Lempiäinen and J. K. Laiho-Steffens, "The performance of polarization diversity schemes at a base station in small/micro cells at 1800 MHz," *IEEE Trans. Veh. Technol.*, vol. 47, no. 3, pp. 1087–1092, Aug. 1998.
[29] L. Lukama, K. Konstantinou, and D. J. Edwards, "Polarization diversity performance for UMTS," in *Proc. Inst. Electr. Eng. Conf Antennas Propag.*, Apr. 2001, vol. 1, pp. 193–197, Publ. No. 480.
[30] M. A. Jensen and M. L. Morris, "Efficient capacity-based antenna selection for MIMO systems," *IEEE Trans. Veh. Technol.*, vol. 54, no. 1, pp. 110–116, Jan. 2005.
[31] A. Paulraj, D. Gore, R. Nabar, and H. Bölcskei, "An overview of MIMO communications—A key to gigabit wireless," *Proc. IEEE*, vol. 92, no. 2, pp. 198–218, Feb. 2004.

David G. Landon (S'06) received the B.S. and M.S. degrees in electrical engineering and the B.A. in German from Brigham Young University (BYU), Provo, UT, in 1999. Currently, he is working towards the Ph.D. degree in electrical engineering at the University of Utah, Salt Lake City, investigating antenna aspects of MIMO communication systems.

From 1998 to 1999, he worked as a Research Assistant at the Telemetering Lab, BYU. From 1999 to 2002, he developed optical time delay reflectometry (OTDR) algorithms for Agilent Technologies, Boeblingen, Germany. Since 2003, he has developed high-rate and direct-sequence spread-spectrum modems and high-rate forward error correction coding for L-3 Communications, Salt Lake City, UT.

Mr. Landon received the Ezra Taft Benson Presidential scholarship for undergraduate studies and the Wayne Brown Fellowship for graduate studies. He received the best undergraduate paper award at the International Telemetering Conference (ITC) in 1999 and second place graduate paper at ITC in 2000.

Cynthia M. Furse (S'85–M'95–SM'99) received the Ph.D. degree from the University of Utah, Salt Lake City, UT, in 1994.

Currently, she is the Director of the Center of Excellence for Smart Sensors, which focuses on imbedded antennas and sensors in complex environments, such as telemetry systems in the human body and sensors for location of faults on aging aircraft wiring, and the Professor/Associate Chair in the Electrical and Computer Engineering Department, University of Utah. She has directed the Utah "Smart Wiring" program, sponsored by Naval Air Systems Command (NAVAIR) and United States Air Force (USAF), since 1998. She is the Chief Scientist for LiveWire Test Labs, Inc., Salt Lake City, UT, a spin off company commercializing devices to locate intermittent faults on live wires. She teaches electromagnetics, wireless communication, computational electromagnetics, microwave engineering, and antenna design.

Dr. Furse was the Professor of the Year in the College of Engineering, Utah State University, for the year 2000, Faculty Employee of the year 2002, a National Science Foundation Computational and Information Sciences and Engineering Graduate Fellow, IEEE Microwave Theory and Techniques Graduate Fellow, and President's Scholar at the University of Utah. She is the Chair of the IEEE Antennas and Propagation Society Education Committee and the Editor-in-Chief of the *International Journal of Antennas and Propagation*.